INSTITUTE OF PLASMA PHYSICS

NAGOYA UNIVERSITY

RESEARCH REPORT

NAGOYA, JAPAN

Experiments of Plasma Confinement in J.I.P.P. Stellarator

II. Convective motions due to trapped particles in stellarator field

Kenro Miyamoto, Akihiro Mohri, Nobuyuki Inoue,
Masami Fujiwara and Kiyoshi Yatsu*

IPPJ-110 OCTOBER 1971

Further communication about this report is to be sent to the Research Information Center, Institute of Plasma Physics, Nagoya University, Nagoya, JAPAN.

* Tokyo University of Education.

Abstract

Dependences of plasma confinement on the properties of the stellarator field such as the rotational transform angle, shear, well depth, the magnitude B as well as the plasma parameters overs a relatively wide range are studied using several kinds of plasma sources. The observed diffusion coefficients are 1/20 $\sim$ 1/30 times the Bohm coefficient. Convective motions of E $\times$ B drift due to the trapped particles at the corners of magnetic surface of the ℓ = 3 stellarator are observed by measuring the distributions of the densities and potentials over the plasma cross section. The magnitude of the observed decay time τ and the scaling law of B and T_e dependences of τ can be explained an order-of-magnitude discussion by the observed convective motions and the low frequency fluctuations observed in the boundary region.

§1. Device and Plasma Sources

A circular $\ell = 3$ stellarator with the major radius of 50 cm and the toroidal field of 4 kG is constructed with good geometrical accuracy[1]. The mold of helical grooves are made by numerically controlled machines. The magnetic surfaces are checked by pulsed electron beam method[2] and they agree well with the calculated ones. The helical winding has a minor radius of 10.6 cm with 8 field periods. Two halves of the stainless steel vacuum vessel with inner radius of 8.4 cm are insulated by ceramic spacers to make ohmic heating method possible. The parameters of magnetic configuration of J.I.P.P. stellarator are shown in Table I. The rotational transform angle is up to 1.7 π and the shear parameter θ is up to 0.15. The well depth is variable from -5 % to +10 %. This device can be used in the torsatron type configuration[3].

We use the plasma sources of a quasi-steady J × B type gun[4] with a fast acting valve, ECRH of 2.45 GHz and ohmic heating[5] by air core coil with the preionization of r f stochastic heating[6]. The J × B type gun produces a plasma with the electron temperature of 1.5 eV and the density of $0.7 \times 10^{10}/cm^3$ in standard conditions. The degree of ionization is ~ 0.5 %. This plasma is in the intermediate collisional regions. The electron temperature can be variable from 0.2 to 2 eV. ECRH plasma is produced by using a magnetron of 2.45 GHz whose electron cyclotron resonant field is 0.87 kG. The microwave power of about 300 W is fed through a coaxial cable and a loop antenna during about 3 ms. Typical ECRH plasma has the electron temperature of 1 eV and the density of $10^{10}/cm^3$. The degree of ionization is about 0.2 %. The electrons are in the intermediate collisional regions while the ions

are in the collisional region. The air core coil for the ohmic heating consists of a homogeneous coil and mirror coils. The winding is arranged so that the disturbance due to the stray field is negligibly small within the plasma region. The afterglow plasma has the electron temperature of 3 eV and the density of $10^{12}/cm^3$. The degree of the ionization is 20 %. This plasma is in the collisional region.

§2. Experimental results using ECRH plasma

Figure 1 shows a typical signal of the ion saturation current of a Langmuir probe. After the power is turned off, the density decreases with two different decay time constants. During about 2 ms after that, the density decays rapidly and then decreases with the decay time of 2 ~ 5 ms. As is shown later, strong convective cells[7] are observed in early period. The time variation of the electron temperature measured by a swept Langmuir probe is also shown in Fig. 1. As the collision time of electron and helium atom is about 4 μs and electron-electron collision time is about 2 μs, the velocity distribution of the afterglow is considered to be nearly maxwellian. With this range of the neutral density and the applied power of 300 W, X rays are not detected by a scintillator and photomultiplier combination and the hot electrons may not exist during the afterglow period.

The dependence of the confinement time of later period on the rotational transform angle and the magnetic well depth are shown in Fig. 2. As it is known how the rotational transform angle, the shear and the plasma radius depend on the ratio of currents of the helical coil to the toroidal field coil, the diffusion coefficient can be estimated from the decay time. The dependence of the diffusion

coefficient on the helical current indicates that the diffusion coefficient appears to relate with the rotational transform angle and not with the shear parameter.

The dependence of the confinement time on the well depth as well as the antiwell depth is weak.

Distributions of the density and the floating potentials over the plasma cross section at different times are measured using a single probe with a scanning mechanism. The reproducibility of the signals are within a few percents. The difference between the floating potential and the plasma potential can be considered to be constant over the plasma cross sections as the electron temperature does not change appreciably except the the boundary and the velocity distribution can be considered to be nearly maxwellian. The direction of the $E \times B$ drift is approximately parallel to the equi-potential lines as the magnetic field is almost perpendicular to the cross section and the magnitude of the field does not change more than $\pm$ 8 % within the plasma region. Therefore the stream-lines of the convective motion are the equi-potential lines themselves. The electrons are trapped at the three corners of the magnetic surface where the magnitudes of the magnetic field are smaller (or the trapped ions diffuse more rapidly) and the potential becomes negative. The convective cells due to these electric fields are observed at the corners. The direction of convective motion is clockwise in these figures. The effect of the enhanced losses due to the convective motion is observed in the corresponding density profile. The decay rate of the density becomes slow as the convective cells fade gradually. Figure 4 shows the profile of the constant $|B|$ surfaces at the position of the different phases of helical coil. The magnitude of the field is small near the separatrix

to which the magnetic surfaces are convex. The distributions of the densities and potentials at the other phase of the helical coil are measured by inverting the direction of the helical current and the similar convective cells are also observed at the corners.

From the similar experiments with the plasma produced by the J × B type gun, we will know whether these characteristics of confinement depend on the plasma properties or on the configuration of magnetic field.

§3. Experimental results using J × B type gun

Figure 5 shows a typical signal of the ion saturation current of the plasma produced by the J × B type gun. The gun is fired at 260 μs after triggering the fast acting valve and is short circuited at 800 μs. The electron temperature of the standard condition is 1.5 eV. The cooling time of the electron by helium gas is about 0.1 sec, but the cooling time of ion by charge exchange with helium atom is estimated to be 0.4 ms. So that the ion temperature during the observed period is low, although the ion energy at the injection stage is high (of the order of 100 eV).

Figure 6 shows the dependence of the confinement time τ of the gun plasma on the rotational transform angle, the well depth and the magnitude B of the field. The dependence of τ on the rotational transform angle is similar to that of ECRH. The dependence on the magnetic well is also weak. The B dependence of τ is linear in our experimental conditions.

Distributions of the density and the floating potential at

different times are shown in Fig. 7. The reproducibility of the signals is very good in the category of gun plasmas and is within several percents. The convective cells at the three corners are again observed. In the case of J × B type gun, the stream lines of convection in the boundary region does not cross the most outside magnetic field. The rapid decay of early period is not observed in contract to the case of ECRH plasma. The convective cells remain even in the later period. The peaks of the density are observed near the centers of the convective cells. It can be considered that the convective cells originates in the property of the magnetic configuration.

§4. Experimental results using ohmic heating plasma

Figure 8 shows the typical signal of the helium plasma produced by ohmic heating using the air core coil with the preionization of r.f stochastic heating. The time variation of the electron temperature is shown in Fig. 8 in the afterglow period.

Figure 9 shows the dependence of the confinement time of ohmic heating plasma on the rotational transform angles ι and the magnitude B of the field. Dependence on ι is similar to those of plasmas mentioned above and B dependence is again linear. The distributions of the density and the potential can not be measured, as the disturbance of the probe during the ohmic heating changes the conditions of plasma production.

§5. Summary

The confinement time τ depends linearly on the magnitude B of the field in the case of the J × B type gun and the ohmic heating. The dependence of τ on the magnetic well depth are weak in the case of ECRH and gun. The relations of the diffusion coefficient on the rotational transform angle are shown in Fig. 10 in three cases of plasmas. The most probable relation is the inverse square dependence on ι. In the lower part of the Fig. 10, the solutions of the density profile of the diffusion equation are plotted with the different diffusion coefficients D, one of which is constant and the other one has inverse linear and inverse square dependence on ι or r^2. The measured density profiles of the plasmas of the ECRH and the gun are plotted and they are similar to the solution with D of inverse square dependence on ι. We can estimate the diffusion coefficient D_1 for the ordinary zeroth order Bessel distribution and the other diffusion coefficient D_3 for the density distribution in the case of $D \propto \iota^{-2}$. The ratios of the ordinary diffusion coefficient D_1 to the Bohm one are 1/13 for ECRH plasma, 1/8 for gun plasma and 1/11 for the ohmic heating plasma. When the diffusion coefficient of D_3 is adopted which is more consistent to the observed one, the ratios are 1/30, 1/20 and 1/27 for the cases of ECRH, gun and ohmic heating respectively.

The magnitude of the observed decay time τ and the scaling law of $\tau \propto T_e/B$ can be explained in order-of-magnitude discussion by the observed convective motion and low frequency fluctuations observed in the boundary region. The electric potential depth of the convective cells are the order of the electron temperature. It may not be proper to apply Galeev-Sagdiev transport theory[8] to the stellarator field in which the electric field with azimuthally varying components due to the

trapped particles are not negligible. We are now studying the behavior of the fluctuation in detail.

Reference

1) K. Miyamoto, A. Mohri, N. Inoue, M. Fujiwara and K. Yatsu: IPPJ - 102 Inst. of Plasma Phys. Nagoya Univ. November 1970.

2) E. Berkl, G. V. Gierke and G. Grieger: IPP 2/69 Garching Juni 1968.

3) C. Gourdon et al: ibid vol. I p847.

4) J. H. Adlam et al: Plasma Physics and Controlled Nuclear Fusion Research, Conference Proc. Novosibirsk, International Atomic Energy Agency, Vienna 1969 vol. I p573.

5) W. Stodiek et al: Plasma Physics and Controlled Nuclear Fusion Research, Conference Proc. Culham, International Atomic Energy Agency, Vienna 1966 vol. II p687.

6) V. N. Bocharov et al: Plasma Physics and Controlled Nuclear Fusion Research, Conference Proc. Novosibirsk International Atomic Energy Agency, Vienna 1969 vol. I p561.

7) S. Yoshikawa et al: ibid vol. I p403.

8) A. A. Galeev and R. Z. Sagdiev: Sov. Phys. JETP 26 233 (1968). T. E. Stringer: Phys. of Fluids 13 810 (1970).

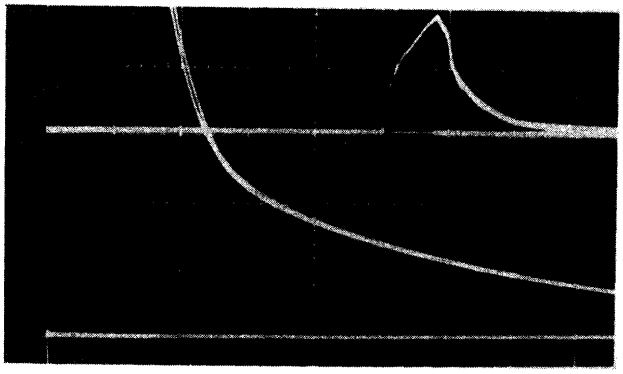

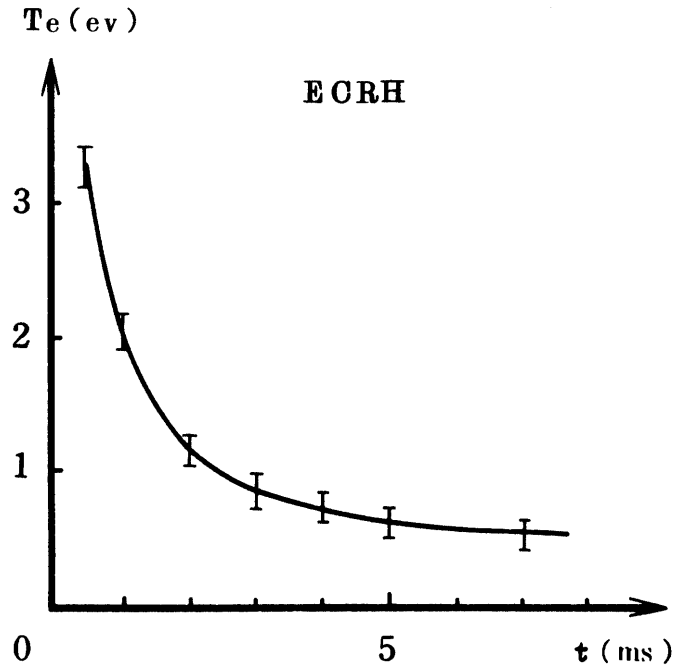

Fig. 1 Typical signal of ion saturation current of ECRH plasma with different sensitivity and time sweep (upper trace: 200 μA/div., 2 ms/div., lower trace: 10 μA/div., 1 ms/div.). The lower figure shows the time variation of the electron temperature.

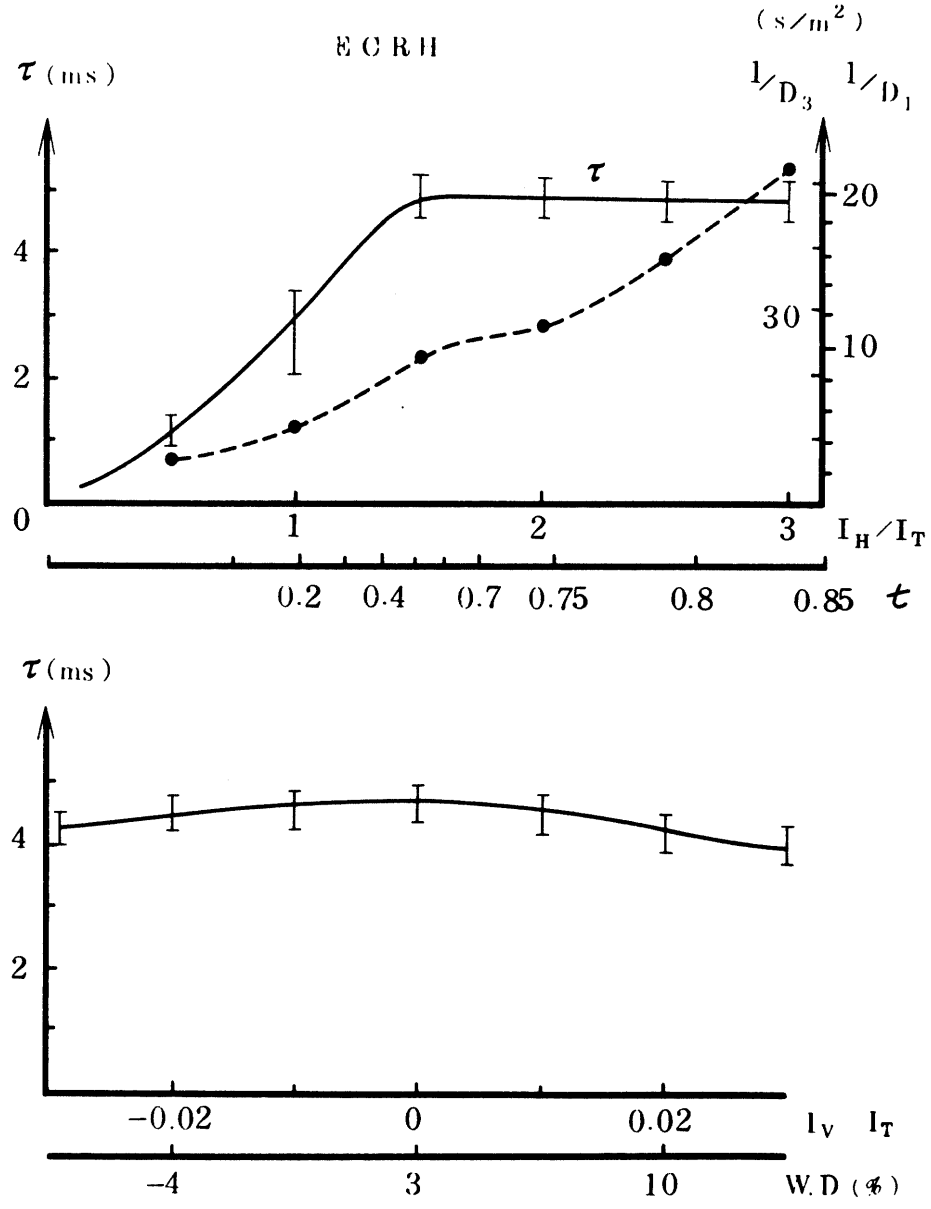

Fig. 2 The upper figure shows the dependence of the confinement time τ on the ratio of currents of the helical coil and the toroidal field coil (the rotational transform angle). The inverse of the diffusion coefficient $1/D_1 = \tau\ (5.8/a^2)$ of the zeroth order Bessel distribution and $1/D_3 = \tau\ (14/a^2)$ of $\rho^2\ J_{-2/3}\ (1.25\ \rho^3)$ distribution are shown in unit of s/m^2. The dependence of the confinement time τ on the magnetic well depth (W.D.) is shown in the lower figure.

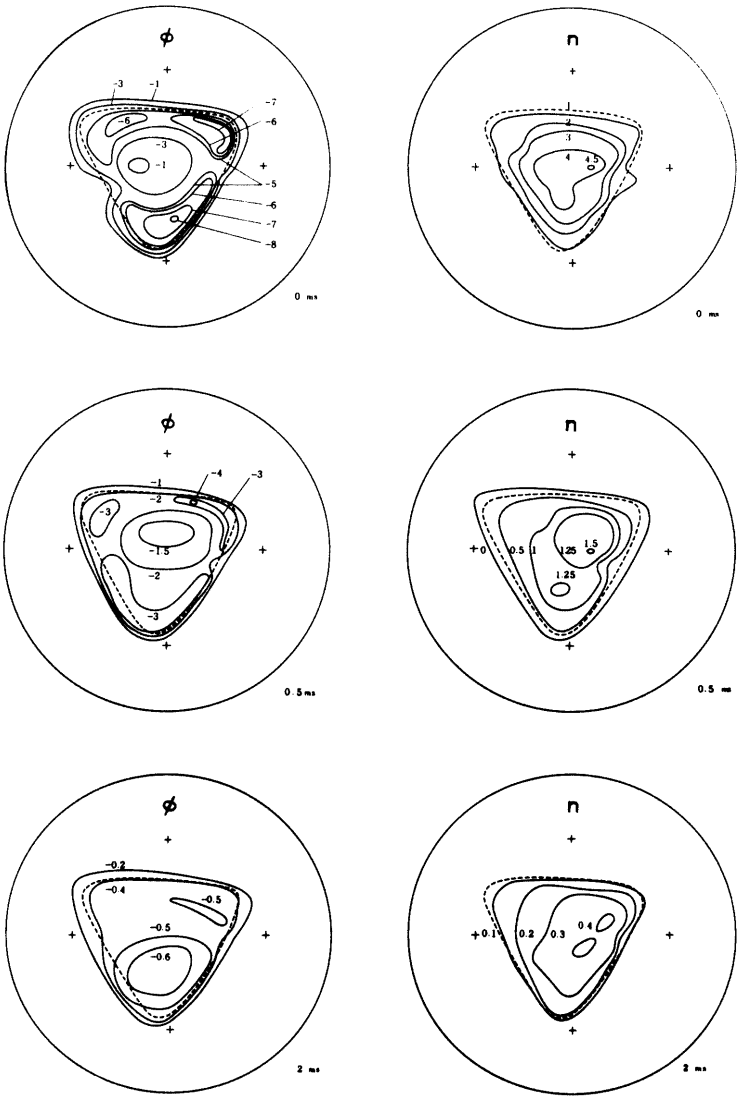

Fig. 3 Two dimensional distributions of the floating potentials (lefthand side) and the densities at different times (0 ms, 0.5 ms and 2 ms after switching off the ECRH power). The numbers in the figures of potential distribution are in volt and the enclosing circle is the inner wall of the vacuum vessel with the diameter of 16.8 cm. The numbers in the figures of density distribution are in arbitrary unit and the magnitude of 1 corresponds approximately to the value of $n\sqrt{Te} \sim 5 \times 10^{10}\sqrt{eV}/cc$. The direction of the magnetic field is backward of the figure.

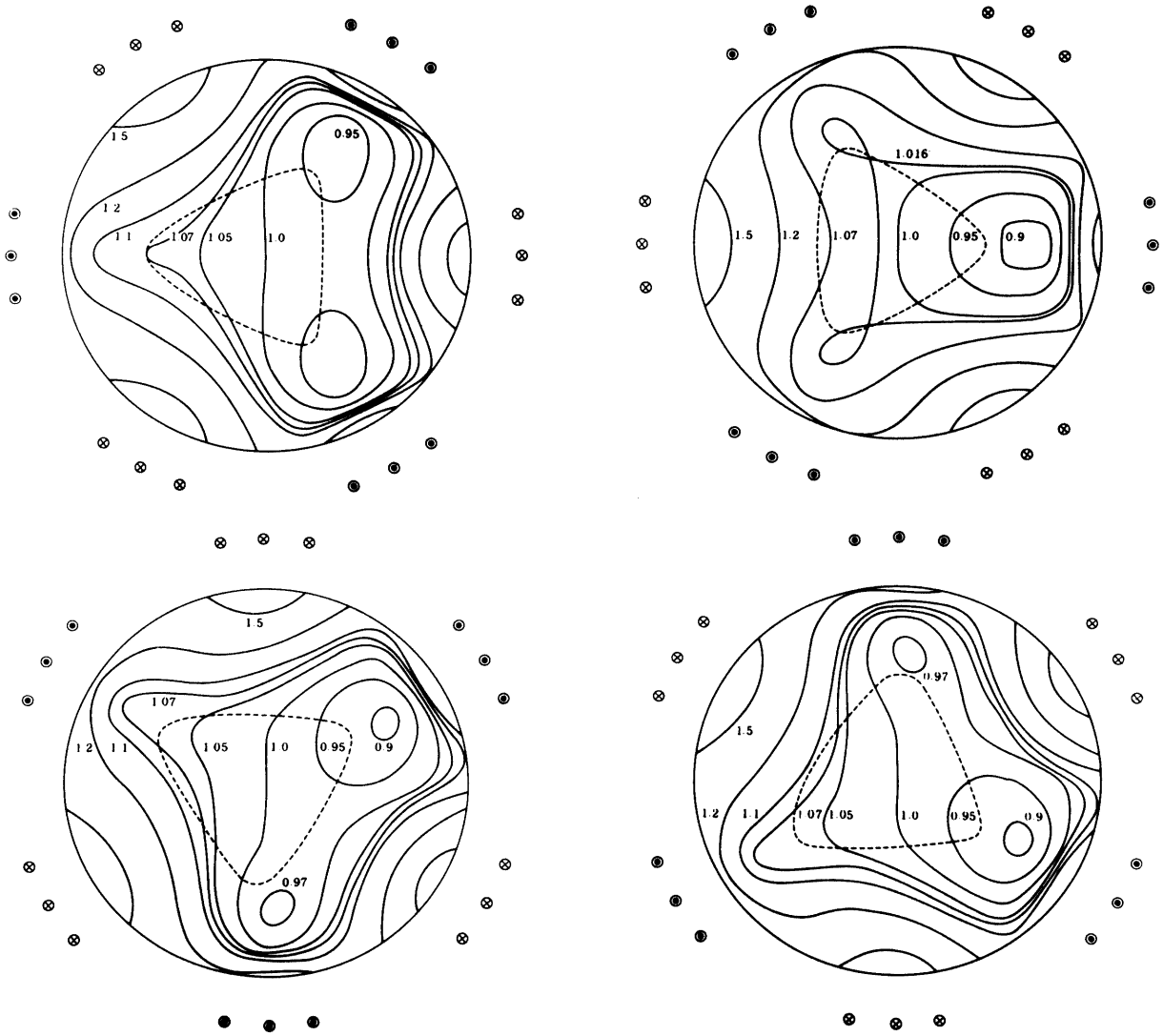

Fig. 4 The constant $|B|$ surfaces of the $\ell = 3$ stellarator field with the magnetic surface (dotted line). The rotational transform angle on the magnetic surface is $1.7\,\pi$.

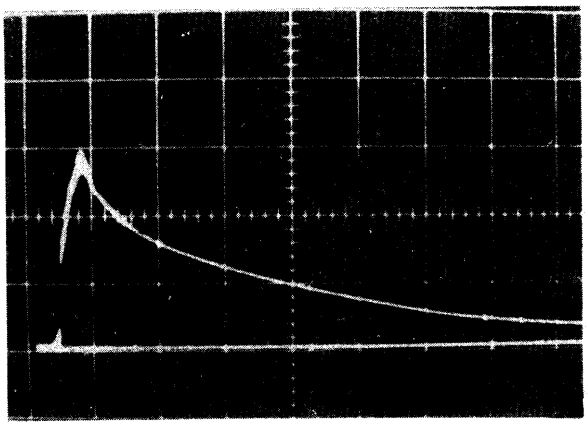

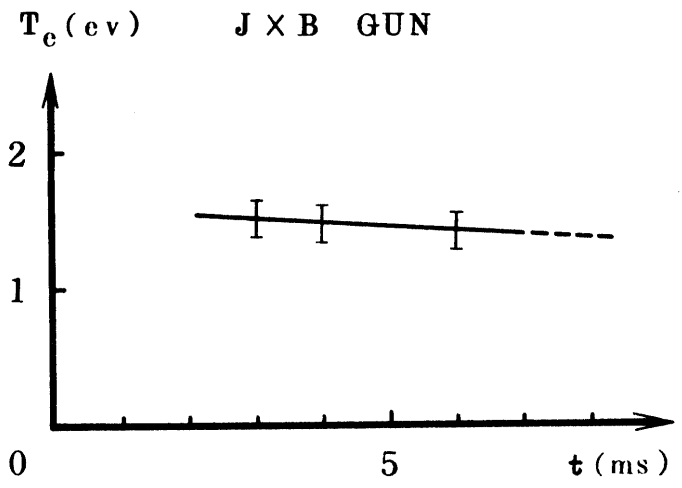

Fig. 5 Typical signal of ion saturation current of the J × B type gun (1 μA/div, 1 ms/div.). The lower figure shows the time variation of the electron temperature.

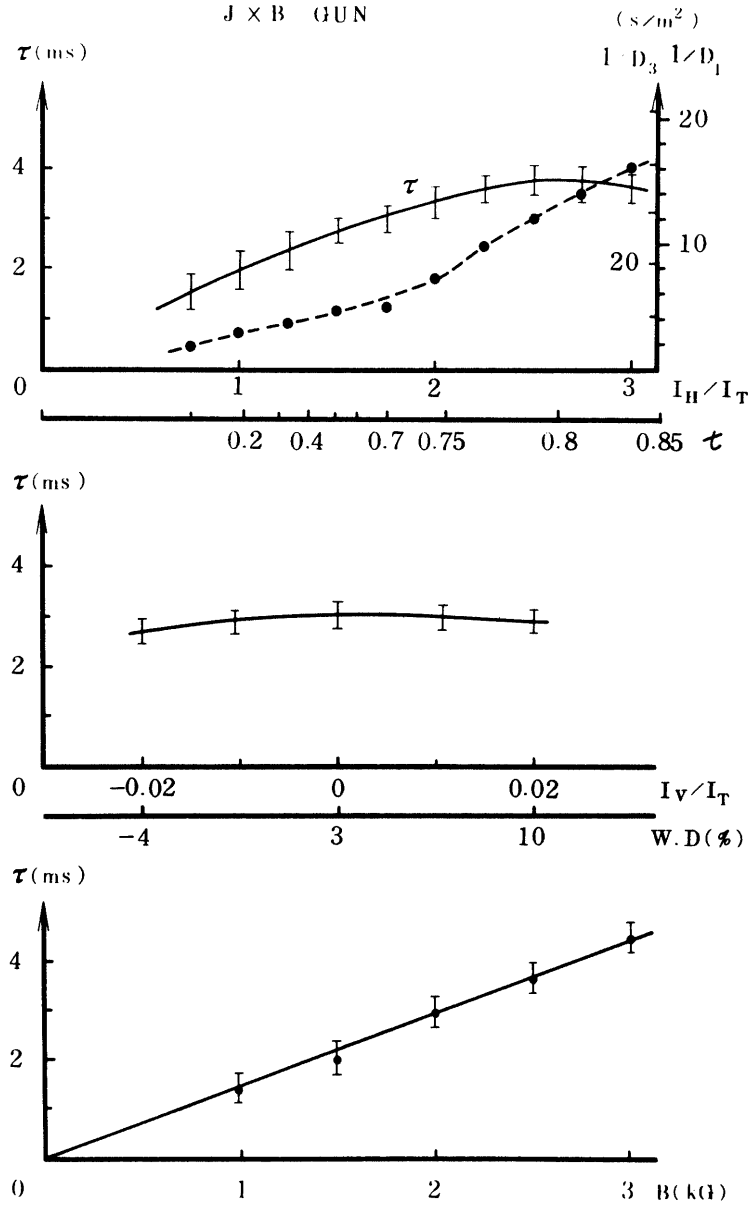

Fig. 6 The dependence of confinement time τ on the rotational transform angle and the well depth (W.D.) is shown when the toroidal field is 2 kG. The dependence of τ on the magnitude B of the toroidal field is also shown when the ratio of currents of helical coil to toroidal field coil is 2. The inverse of the diffusion coefficient $1/D_1$ and $1/D_3$ are given in the top figure.

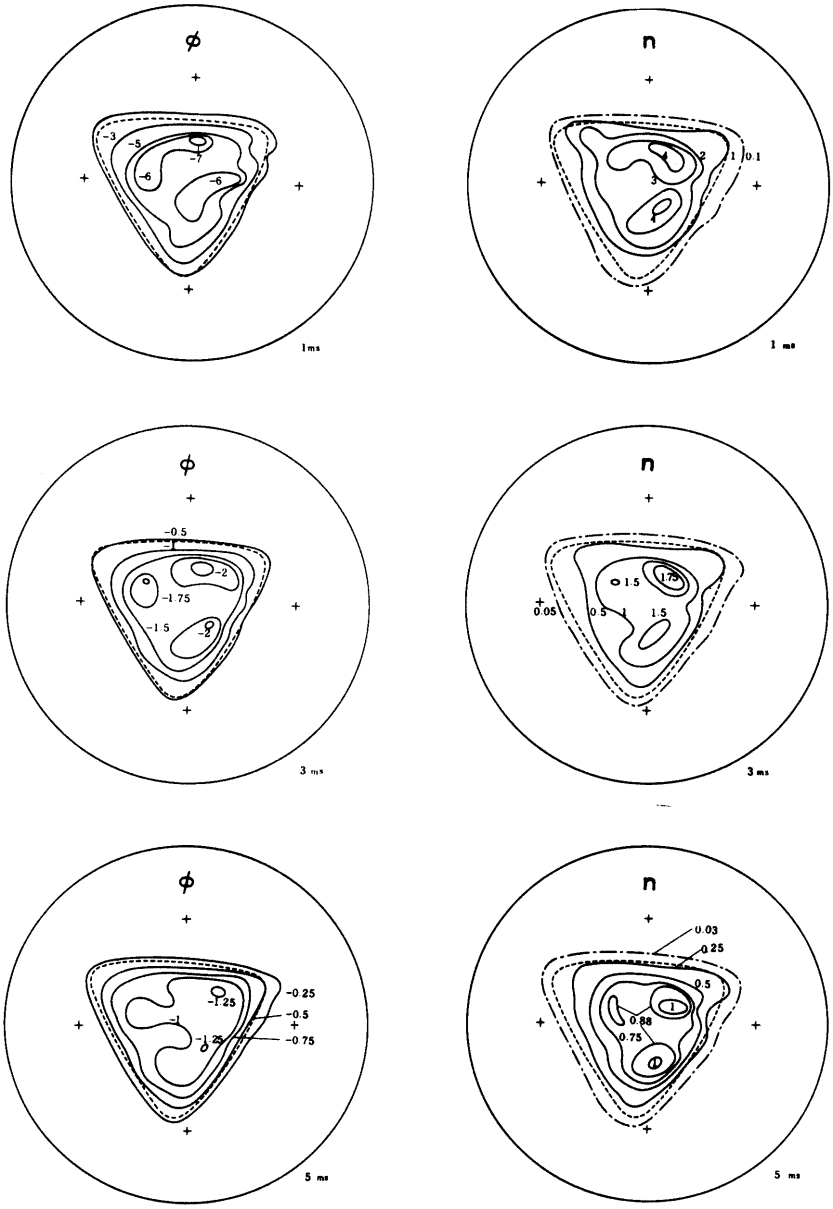

Fig. 7 Two dimensional distributions of the floating potentials (lefthand side) and the densities at different times (1 ms, 3 ms and 5 ms after triggering the fast acting valve). The numbers in the figures of potential distribution are in volt and the enclosing circle is the inner wall of the vacuum vessel with the diameter of 16.8 cm. The numbers in the figures of density distribution are in arbitrary unit and the magnitude of 1 corresponds approximately to the value of $n\sqrt{Te} \sim 3 \times 10^9 \sqrt{eV}/cc$. The direction of the magnetic field is backward of the figure.

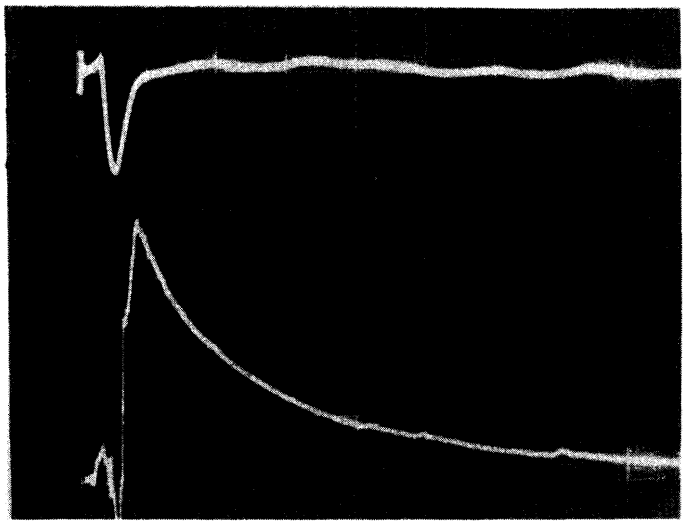

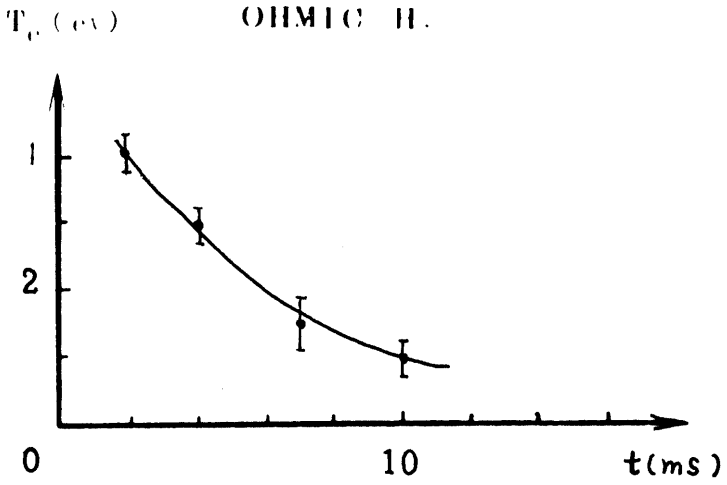

Fig. 8 Typical signal of ion saturation current of afterglow plasma produced by ohmic heating (lower trace). The sensitivity is 100 μA/div. and time sweep is 2 ms/div. The upper trace is the induced current in the plasma (130 A/div.). The lower figure shows the time variation of the electron temperature.

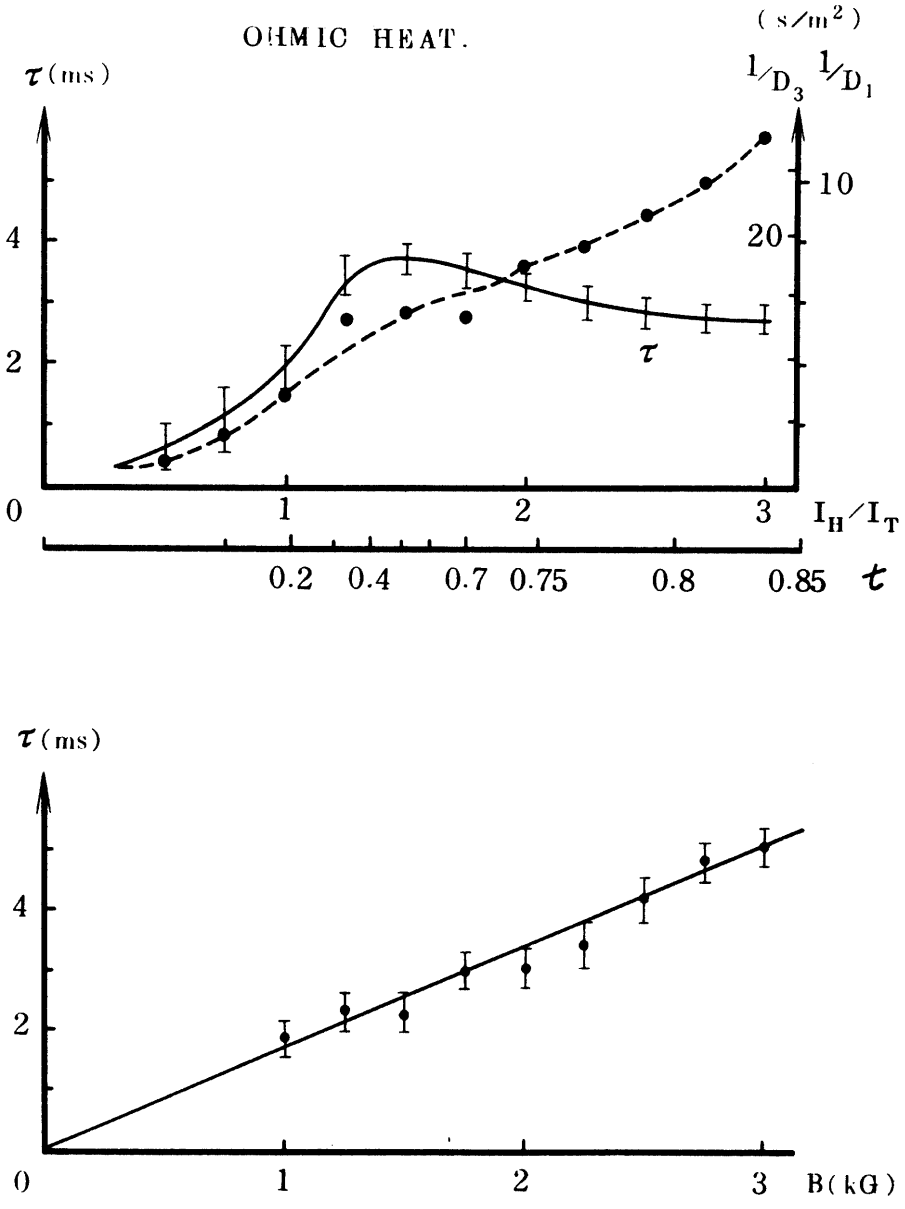

Fig. 9 The upper figure shows the dependence of the confinement time τ on the rotational transform angle when the toroidal field is 2 kG. The dependence of τ on the magnitude B of the toroidal field is shown in the lower figure when the ratio of helical current to toroidal one is kept to be 2. The inverses of the diffusion coefficients $1/D_1$ and $1/D_3$ are also shown.

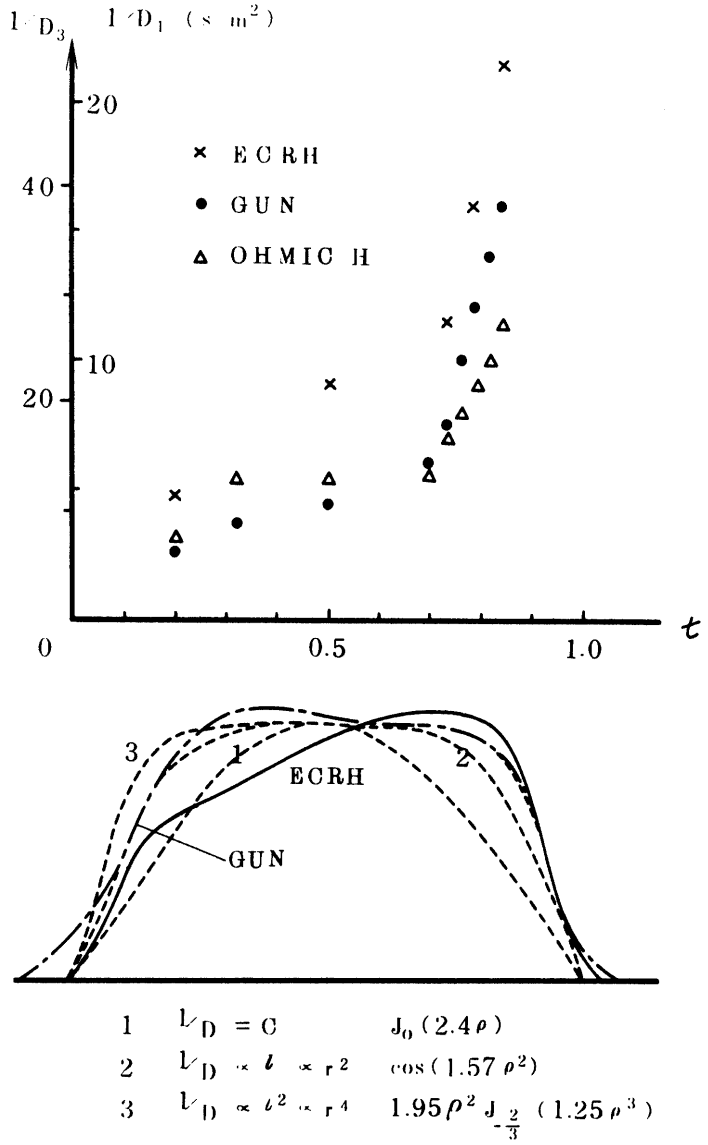

Fig. 10 Dependence of the confinement time on the rotational transform angle in the case of ECRH plasma (B = 0.87 kG, Te ~ 0.8 eV), the plasma produced by J × B type gun (B = 2 kG, Te ~ 1.5 eV) and ohmic heating plasma (B = 2 kG, Te ~ 3 eV). The inverse of the diffusion coefficient $1/D = \tau\ (5.8/a^2)$ of the zeroth order Bessel distribution of the density and $1/D_3 = \tau\ (14/a^2)$ of $\rho^2\ J_{-2/3}\ (1.25\rho^3)$ distribution are shown. The density profile of $J_0(2.4\ \rho)$, cos $(1.57\ \rho^2)$ and $\rho^2\ J_{-2/3}\ (1.25\ \rho^3)$ are solutions of the diffusion equation with D = const, $D \propto \iota^{-1} \propto r^{-2}$ and $D \propto \iota^{-2} \propto r^{-4}$ respectively. The density profile of the plasma of ECRH and the J × B type gun are shown.